An Organic Radical Solid Solution with Strong Ferromagnetic Exchange

Hidenori Murata,† Joel T. Mague,‡ Safo Aboaku,† Naoki Yoshioka,§ and Paul M. Lahti*,†

Department of Chemistry, University of Massachusetts, Amherst, Massachusetts 01003, Department of Chemistry, Tulane University, New Orleans, Louisiana 70118, and Department of Applied Chemistry, Keio University, Yokohama 223-8522, Japan

Received April 27, 2007
Revised Manuscript Received June 22, 2007

Organic molecular magnetism has advanced significantly in the past decade[1] with improved recognition of crystallographic packing motifs that give predictable, or at least rationalizable, exchange between unpaired spins. Hydrogen bonding in radicals has been particularly promising, giving some control over intermolecular geometric relationships that affect the subtle interplay of unpaired spins in a solid.[2] Mixed crystals and materials offer even wider possibilities for creating and influencing new electronic properties in ways that are not possible in single-component systems. In this article, we report an unusual, solid-solution crystallization of two organic radicals to give strong 1D chain ferromagnetic exchange that is mostly controlled by hydrogen-bonding assembly of the radicals.

Yoshioka and co-workers[3] showed that hydrogen-bonded chains in the benzimidazole group assemble nitronylnitroxide radical groups in BImNN into "T-stacks" that favor ferromagnetic exchange by a through-space spin polarization (SP) model. Figure 1 shows the interaction between close contact sites of appreciable spin density in this arrangement. Favorable contacts occur when spin orbitals of opposite spin density overlap, leading in the case of BImNN to ferromagnetic (FM) exchange. Magnetic measurements support[3−4] the SP model, showing 1D Heisenberg chain ferromagnetic (FM) exchange in BImNN.

Murata et al. reported[5] that the fluorinated analogue of BImNN, F4BImNN, forms a surprisingly similar crystal structure to that of BImNN. The hydrogen bonding in

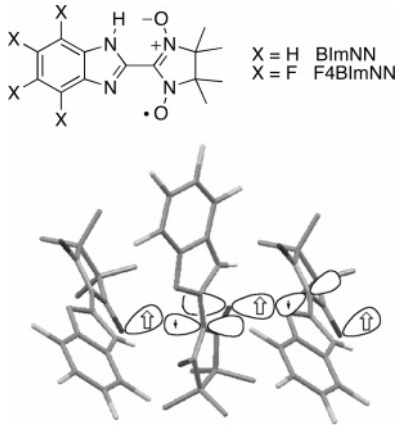

Figure 1. T-stack spin site contacts give 1D ferromagnetic chain exchange behavior by favorable spin overlap.

F4BImNN remains sufficiently strong to assemble virtually identical chains to those in BImNN. Notably, the magnetism of F4BImNN above 2 K is also quite similar to that of BImNN, and fits 1D Heisenberg chain FM exchange with $J_{1D} = +17$ K. The crystallographic scaffold imposed by the benzimidazole hydrogen bonding appears to control the magnetism in both of these materials.

Fluorinated and unfluorinated compounds can cocrystallize in motifs that do not form in the single-component crystals.[6] BImNN and F4BImNN were recrystallized from a 1:1 mol:mol ratio solution to test whether they would cocrystallize. Deep blue-black needles formed, which thin layer chromatography and mass spectrometry showed to incorporate both radicals. Quantitative HPLC of a visually single crystal showed a 46:54 mol:mol ratio of F4BImNN:BImNN. Differential scanning calorimetric measurements of the mixture showed a decomposition exotherm at 199 °C, whereas F4BImNN decomposes at 170 °C, and BImNN at[3a] 217−219 °C. If the product mixture were substantially heterogeneous, it should show decomposition points for the components instead of (or, in addition to) one different from both.

X-ray diffraction (XRD) analysis of several single crystals of the mixture confirmed that the fluorinated and nonfluorinated radicals intimately co-mingle. The analysis[7] of one crystal at 100 K is summarized in Table 1, with molecular and intermolecular structure data given in Table 2. The reflection data showed a mosaic spread of 0.6°, indicating that crystal does not have heterogeneous diffraction regions. The analysis showed the crystal to incorporate fluorinated and unfluorinated benzimidazole rings randomly into a

* Corresponding author. E-mail: lahti@chem.umass.edu.
† University of Massachusetts.
‡ Tulane University.
§ Keio University.

(1) (a) Kahn, O. *Molecular Magnetism*; VCH: New York, 1993. (b) Lahti, P. M. *Magnetic Properties of Organic Materials*; Marcel Dekker: New York, 1999. (c) Itoh, K.; Kinoshita, M. *Molecular Magnetism: New Magnetic Materials*; Gordon and Breach: Newark, NJ, 2000. (d) Palacio, F.; Markova, T. *Carbon-Based Magnetism: An Overview of the Magnetism of Metal-Free Carbon-Based Compounds and Materials*; Elsevier: Amsterdam, 2006.

(2) Lahti, P. M. Magneto-structural correlations in π-conjugated nitroxide-based radicals: hydrogen-bonds and related interactions in molecular organic solids. In *Carbon-Based Magnetism: An Overview of the Magnetism of Metal-Free Carbon-Based Compounds and Materials*; Palacio, F., Markova, T., Eds.; Elsevier: Amsterdam, 2006; p 23*ff*.

(3) (a) Yoshioka, N.; Irisawa, M.; Mochizuki, Y.; Aoki, T.; Inoue, H. *Mol. Cryst. Liq. Cryst., Sect. A* **1997**, *306*, 403. (b) Yoshioka, N.; Irisawa, M.; Mochizuki, Y.; Kato, T.; Inoue, H.; Ohba, S. *Chem. Lett.* **1997**, 251. (c) Yoshioka, N.; Inoue, H. Crystal control in organic radical solids. In *Magnetic Properties of Organic Materials*; Lahti, P. M., Ed.; Marcel Dekker: New York, 1999; p 553.

(4) Sugano, T.; Blundell, S. J.; Hayes, W.; Day, P. *Polyhedron* **2003**, *22*, 2343.

(5) Murata, H.; Delen, Z.; Lahti, P. M. *Chem. Mater.* **2006**, *18*, 2625.

(6) Cf., for example, (a) Thalladi, V. R.; Weiss, H.-C.; Blaeser, D.; Boese, R.; Nangia, A.; Desiraju, G. R. *J. Am. Chem. Soc.* **1998**, *120*, 8702. (b) Krafft, M. P.; Giulieri, F.; Fontaine, P.; Goldmann, M. *Langmuir* **2001**, *17*, 6577. (c) Dunitz, J. D.; Gavezzotti, A.; Schweizer, W. B. *Helv. Chim. Acta* **2003**, *86*, 4073. (d) Sada, K.; Inoue, K.; Tanaka, T.; Epergyes, A.; Tanaka, A.; Tohnai, N.; Matsumoto, A.; Miyata, M. *Angew. Chem., Int. Ed.* **2005**, *44*, 7059. (e) Awwadi, F. F.; Willett, R. D.; Peterson, K. A.; Twamley, B. *Chem.—Eur. J.* **2006**, *12*, 8952.

(7) Crystallographic analysis carried out with SHELXL97; Sheldrick, G. *SHELXTL97 Program for the Refinement of Crystal Structures*; University of Göttingen: Göttingen, Germany, 1997. Bonding parameters and intermolecular contact summary from PLATON; Spek, A. L. *J. Appl. Cryst.* **1988**, *21*, 578. ORTEP diagrams with ORTEP-III for Windows; Farrugia, L. J. *J. Appl. Cryst.* **1997**, *30*, 565. Additional diagrams made with Mercury 1.4.2 software from the Cambridge Crystallographic Data Centre.

10.1021/cm0711459 CCC: $37.00
Published on Web 07/25/2007

Table 1. Crystal Data and Structure Refinement for Alloy System

empirical formula	$C_{28}\,H_{30}\,F_4\,N_8\,O_4$
fw	618.60 (1:1 F4BImNN:BImNN)
T (K)	100(2)
wavelength (Å)	0.71073
cryst syst	orthorhombic
space group	*Pbca*
a (Å)	*8*.694(3)
b (Å)	15.491(4)
c (Å)	20.569(6)
V (Å^3)	2770.2(14)
α (deg)	90
β (deg)	90
γ (deg)	90
Z	4
D_{calcd} (g/cm^3)	1.483
abs coeff (mm^{-1})	0.120
F(000)	1288
cryst size (mm^3)	0.25 × 0.09 × 0.03
θ range for data collection (deg)	1.98−23.31
index ranges	$-9 \le h \le 9$, $-17 \le k \le 17$, $-22 \le l \le 22$
no. of reflns collected	15 925
no. of independent reflns	2003 [R(int) = 0.0808]
completeness to $\theta = 23.31°$ (%)	100.0
abs correction	semiempirical from equivalents
max. and min. transmission	0.9962 and 0.9705
refinement method	full-matrix least-squares on F^2
data/restraints/params	2003/168/221
GOF on F^2	1.136
final R indices [$I > 2\sigma(I)$]	$R_1 = 0.0663$, $wR_2 = 0.1541$
R indices (all data)	$R_1 = 0.0839$, $wR_2 = 0.1638$
largest diff. peak and hole (e Å^3)	0.332 and −0.281

Table 2. Comparison of F4BImNN, BImNN, and Alloy System

	F4BImNN[a]	BImNN	alloy
r([N)O┅C), T-stack (Å)	3.139(4)	3.17(3)[b]	3.077(4)
r([N)H┅O(N)), H-bond (Å)	2.01	1.99[b]	1.90
r([N)H┅N), H-bond (Å)	2.75	2.77[b]	2.72
∠([N)H···O−N), H-bond angle (deg)	55.1	148.4[b]	158.0
∠([N)H···N═C), H-bond angle (deg)	110.2	105.3[b]	110.1
BIm-NN torsion (deg)	22.1(5)	23(4)[b]	20.1(5)
J_{1D}, K (cm^{-1})	17 (11.8)	22[c] (15.3)	15.1 (10.5)

[a] See ref 5. [b] See ref 3b. [c] See ref 4.

common lattice as a solid solution or alloy. In such materials, a large amount of a dopant compound or ion can occupy numerous, random lattice sites in a material, retaining one overall lattice with varying composition.[8] The ORTEP style picture shown in Figure 2 shows one ring fluorinated and one nonfluorinated for ease of reference to Table 2, but the analysis does not distinguish specific lattice positions for each radical.

Figure 2 shows two important intermolecular contacts in the lattice: the N2−H2n···O2−6 hydrogen-bonding interaction (dashed bond), and the N3O1···C8−6 T-stack contact (arrow). The N2−H2n···O2−6 hydrogen bond is nonlinear, like that in F4BImNN[5] and BImNN[3b] (Table 2), but is reinforced by a somewhat long N2H2n···N1−6 hydrogen-bond-like interaction. The hydrogen bonds assemble the radicals into 1D chains of T-type stacks in the motif of Figure 1. These are very similar to those in the pure component radicals, as shown by the comparisons in Table 2. These 1D chains induce the main exchange interaction between unpaired spins in the lattice. This occurs at the N3O1···C8−6 contact (r[O1···C8−6] = 3.077(4) Å) in the T-stack, where the major spin densities of the nitronylnitroxide radicals are FM aligned as shown in Figure 1. These contacts therefore should induce ferromagnetic exchange along the whole chain of T-stacks, based on qualitative spin orbital overlap. Computational analysis of the very similar F4BImNN 1D chain T-stack arrangement shows high-spin FM exchange in agreement with experiment.[5]

Dc paramagnetic susceptibility χ of the alloy was measured, using the HPLC-determined ratio of F4BImNN:BImNN as average molecular weight. A χT vs T plot at lowest field (Figure 3) shows the characteristic low-temperature upturn of ferromagnetic exchange. The downturns at higher fields are due to easy saturation, shown in the magnetization vs field inset of the figure. This is also seen in BImNN[4] and F4BImNN[5] due to the strong chain exchange. Similarly to BImNN[3] and F4BImNN,[5] the magnetization vs field plot lies well above the theoretical $S = 1/2$ curve, close to that expected for an effective $S = 11$.

A nonlinear least-squares fit of the 1000 Oe data to a 1D Heisenberg chain model[9] with spin Hamiltonian $H = -2J\sum S(i)S(j)$ gives $J_{1D} = +15.1 \pm 0.2$ K, and a mean field constant $\theta = 0.34 \pm 0.02$ K; the uncertainties are statistical 95% confidence limits. These results are in good accord with

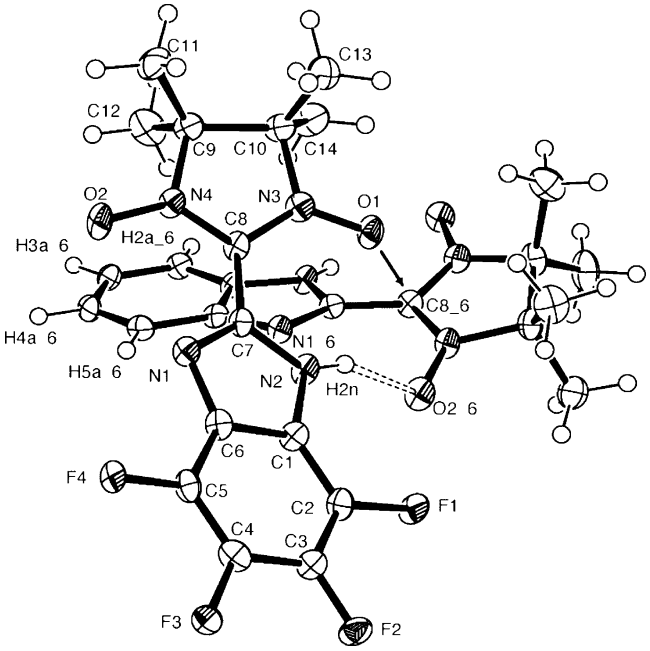

Figure 2. ORTEP style diagram for alloy crystal of F4BImNN/BImNN, showing two molecules generated by ($x + 1/2$, y, $-a + 1/2$) symmetry operation. Ellipsoids shown at the 50% probability level. Fluorine and hydrogen atom positions on the benzenoid rings are actually random in solved crystal structure, but are shown on separate rings to reflect the actual molecular structures. The NH···ON hydrogen bond is shown as a dashed bond, the NO···C "T-stack" contact is shown by the arrow.

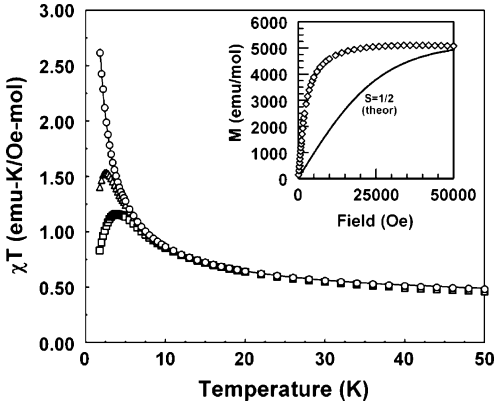

Figure 3. χT vs T plots for polycrystalline F4BImNN/BImNN alloy at 1000 (○), 5000 (△), and 10 000 (□) Oe. Solid line shows fit to a 1D Heisenberg ferromagnetic chain model (see text for details). Inset shows molar magnetization (M) vs field (H) data at 1.8 K (○), and theoretical $M(H)$ curve for $S = 1/2$.

(8) Cf. Callister, W. D., Jr. *Materials Science and Engineering: An Introduction*, 7th ed.; John Wiley & Sons: New York, 2006.

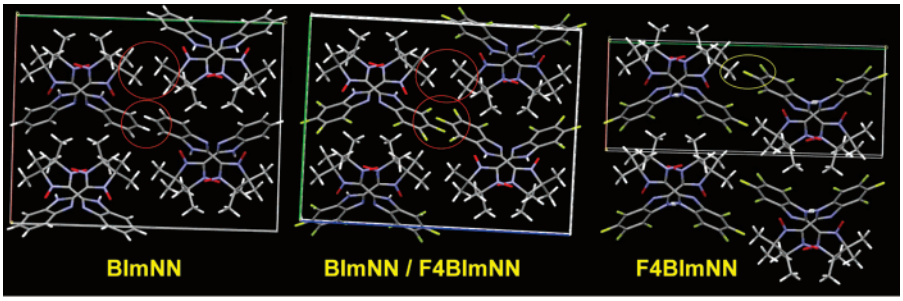

Figure 4. Interchain contacts in BImNN, the alloy, and F4BImNN; chains run into the figure, which shows the *ab*-plane for BImNN, *bc*-plane for the alloy, and *ab*-plane for F4BImNN. Red circles show methyl−methyl and aryl−aryl interactions, yellow circle shows methyl−(F−C aryl) interactions.

SP expectation for a ferromagnetically coupled chain of $S = 1/2$ molecules and are compared to the results obtained for the separate pure components of the mixture in Table 2. Thus, the magnetostructural relationship first shown for BImNN and reproduced in F4BImNN is maintained even in a solid solution, because the placement of spins and spin density is so similar.

Sharmin et al.[10] reported that BImNN solid EPR spectra exhibit peak-shape changes and decreasing average *g*-values at low temperature, consistent with systems having strongly uniaxial exchange. F4BImNN also exhibits peak-shape changes and decreasing average *g*-value as temperature drops. Although the powdered mixture also shows line shape changes, its average *g*-value increases as the temperature drops (see the Supporting Information).

The F4BImNN and BImNN radicals are nearly interchangeable in the alloy lattice because of their similar shape and volume. From their separate crystal structures, the molecular volumes for F4BImNN and BImNN are 285.4 and 265.9 Å^3, respectively.[11] Comparable unit-cell volumes for the two are 3010.8 and 2732.4 Å^3, using two unit cells for BImNN to maintain the same number of molecules per unit volume.

Although this mixture of F4BImNN/BImNN behaves as a solid solution alloy, it must be noted that the phase diagram of this two-component system has not yet been explored over a range of composition. In particular, pure F4BImNN and BImNN have subtly different crystal structures, despite their similarities of molecular conformation and crystal chain formation. Figure 4 compares contacts between 1D hydrogen-bonded chains in F4BImNN, BImNN, and the alloy. F4BImNN exhibits close contacts between methyl groups in the nitronylnitroxide and F−C groups on the aryl ring; the strong electronegativity of the F−C groups makes these favorable dipolar contacts. BImNN, by contrast, exhibits methyl−methyl and aryl−aryl (CH···HC) close contacts. The alloy lattice more closely resembles the BImNN lattice. Presumably, at some composition range for mixing the two, there should be a change from the F4BImNN type to BImNN type lattice, or heterogeneous crystallization of different lattice types (phase separation of the solid solution).

Neutral constituent organic magnetic alloys have not been much explored.[12] Mukai and co-workers studied alloys of verdazyl radicals by powder XRD, EPR, and magnetism.[13] Their magnetic behaviors vary by mixture components and composition. But, their detailed crystallographic structures are not available. In the present case, the alloy lattice has been clearly determined.

F4BImNN and BImNN are electrostatically more different than the verdazyl alloy components. As in the verdazyl cases, the similar size and shape of BImNN and F4BImNN assist alloy formation, but their directional NH···ON hydrogen-bond formation add a crucial new element for assembling them into T-stacks for FM exchange, despite the difference in electrostatic natures of their benzimidazole rings. Still, the balance of effects controlling the packing can be subtle. Yoshioka and co-workers have shown that modest structural changes to BImNN can give significant changes in solid-state crystal packing and magnetic-exchange behavior.[14] Phase diagram studies for F4BImNN/BImNN mixtures are planned to determine possible variations of their crystallography as a function of composition.

Acknowledgment. Work at UMass−Amherst was supported in part by the U.S. National Science Foundation under Grants CHE 0415716 (H.M., S.A., P.M.L.), CHE-0443180 (EPR facility), and CTS-0116498 (Nanomagnetics Facility). J.T.M. thanks the Louisiana Board of Regents through the Louisiana Educational Quality Support Fund (Grant LEQSF (2003-2003)-ENH-TR-67) for the purchase of a diffractometer and the Tulane University Chemistry Department for support of its X-ray diffraction facility. Research at Keio University was partly supported by a Grant-in-Aid for Exploratory Research 16651070 of the Ministry of Education, Culture, Sports, Science and Technology (MEXT). We thank Yilin Qiu for HPLC assistance.

Supporting Information Available: Details of sample preparation, crystallographic analysis (CIF file also deposited with Cambridge Structural Database, #651221), HPLC and mass spectra of mixture samples, details of magnetic data analysis, neat powder EPR spectra and *g*-values for polycrystalline F4BImNN and the alloy, FTIR spectra for the component radicals and alloy (PDF). This information is available free of charge on the Internet at http://pubs.acs.org.

CM0711459

(9) (a) Baker, G. A., Jr.; Rushbrooke, G. S.; Gilbert, H. E. *Phys. Rev. A* **1964**, *135*, 1272. (b) Swank, D. D.; Landee, C. P.; Willet, R. D. *Phys. Rev. B* **1979**, *20*, 2154.

(10) Sharmin, S.; Blundell, S. J.; Sugano, T.; Ardavan, A. *Polyhedron* **2005**, *24*, 2360.

(11) *Spartan Build 119 for Irix 6.5*; Wavefunction, Inc.: Irvine, CA, 2002.

(12) Charge transfer mixed organic magnetic materials, by comparison, have been much studied. As general references, see: (a) Miller, J. S.; Epstein, A. J. *MRS Bull.* **2000**, *25*, 21. (b) Miller, J. S.; Epstein, A. J. *Adv. Chem. Series* **1995**, *245*, 161.

(13) (a) Mukai, K.; Suzuki, K.; Ohara, K.; Jamali, J. B.; Achiwa, N. *J. Phys. Soc. Jpn.* **1999**, *68*, 3078. (b) Jamali, J. B.; Achiwa, N.; Mukai, K.; Suzuki, K.; Asano, T.; Ajiroy, Y.; Matsuda, K.; Iwamura, H.; Kuwajima, S.; Soejima, Y. *Mol. Cryst. Liq. Cryst.* **1999**, *334*, 121. (c) Mukai, K.; Yanagimoto, M.; Shimobe, Y.; Inoue, K.; Hosokoshi, Y. *Chem. Phys. Lett.* **1999**, *311*, 446. (d) Mukai, K.; Yanagimoto, M.; Narimatsu, S.; Maruyama, H.; Narumi, Y.; Kindo, K. *J. Phys. Soc. Jpn.* **2002**, *71*, 2539.

(14) (a) Nagashima, H.; Hashimoto, N.; Inoue, H.; Yoshioka, N. *New J. Chem.* **2003**, *27*, 805. (b) Nagashima, H.; Inoue, H.; Yoshioka, N. *Polyhedron* **2003**, *22*, 1823. (c) Nagashima, H.; Fujita, S.; Inoue, H.; Yoshioka, N. *Cryst. Growth Des.* **2004**, *4*, 19. (d) Nagashima, H.; Inoue, H.; Yoshioka, N. *J. Phys. Chem. B* **2004**, *108*, 6144.